

The Photo-Absorption and Surface Feature of Nano-Structured TiO₂ Coatings

¹Maryamossadat Bozorgtabar, ²Mohammadreza Rahimipour, ³Mehdi Salehi, and ⁴Mohammadreza Jafarpour

Abstract—Titanium dioxide coatings were deposited by utilizing atmospheric plasma spraying (APS) system. The agglomerated nano-powder and different spraying parameters were used to determine their influences on the microstructure surface feature and photo-absorption of the coatings. The microstructure of as-sprayed TiO₂ coatings were characterized by scanning electron microscope (SEM). Surface characteristics were investigated by Fourier Transform Infrared (FT-IR). The photo absorption was determined by UV-VIS spectrophotometer. It is found that the spray parameters have an influence on the microstructure, surface feature and photo-absorption of the TiO₂ coatings.

Keywords—APS, TiO₂, Nanostructured Coating, Photo-absorption

1. INTRODUCTION

NANO-CRYSTALLINE TiO₂ has been investigated extensively in recent years because of its many potential applications; in particular, the utilizations in photo-catalysis e.g. for the purification of air and water from contaminants in photoelectrical cells or as gas sensors appear to be very attractive [1-4]. These processes are based on the feature that TiO₂ is able to photo-catalysis many organic substances under UV irradiation. It is generally assumed that electrons and holes created by the absorption of an UV photon may oxidize or reduce any species adsorbed at the surface of nano-crystalline TiO₂ [5, 6]. Since the surface plays a dominant role in those applications, the nano-scale dimension is instrumental in facilitating many new technological approaches. Usually, the size, surface feature and morphology have been found to be critical parameters in determining their suitability for particular applications [7, 8]. Many techniques have been developed for depositing TiO₂ catalysts on to a solid substrate, for example, dip coating from suspension, spray coating, sputtering, sol-gel-related methods and electrophoresis deposition [9-11]. Also, different types of substrates have been tested; for example, glass beads, glass tubes, fiberglass, quartz, stainless steel, aluminum, activated carbon, and silica [12, 13]. Nowadays, thermal spraying is widely used to prepare TiO₂ coatings for mechanical and biomedical applications due to their hardness, wear and corrosion and bio-compatibility behavior [14, 15].

The studies performed in the last few years showed that the thermal spray technique could be employed to obtain TiO₂ coatings with an effective photo-catalytic performance for the decomposition of organic compounds [16]. In thermal spraying, the material feedstock (commonly a powder with typical particles size distribution ranging from 10 to 100 μm) is injected in an enthalpic source (thermal plasma or flame obtained by ionization-excitation of inert gases or combustion, respectively). The particles are melted, or partially melted, and subsequently accelerated by the gas flow and impacted on the target substrate where rapid solidification and deposit build-up occurs. The air plasma spray (APS) process has been used for many years to form TiO₂ and other ceramic oxide coatings. This APS process is preferred due to the high temperature of the plasma jet which is necessary to thermally spray high melting point materials effectively [17]. During the thermal spraying of ceramic oxides it is necessary to totally or partially melt the powder particles to make coatings. Plasma-spraying technique is an economical and versatile fabrication process for producing large surface coatings with almost unlimited types of materials. The coatings thickness, texture and bonding strength can be controlled easily through spraying parameters, powder matrix and substrate state [18-21]. In this research, the coatings were deposited through atmospheric plasma spray using different argon flow rates and spray distances and using TiO₂ nano-powders containing anatase and rutile as feedstock. The influence of the Argon flow rate and spray distance on the morphology, photo absorption energy and surface characteristics of the coating were investigated.

II. MATERIALS AND EXPERIMENTAL PROCEDURES

A. Materials

P25/20 nano-structured TiO₂ powders were employed in this study. Feedstock powder was commercially granulated nanopowders containing anatase and rutile phase. The average size diameter of the agglomerated particles was about 20 μm. Stainless steel plate was employed as a substrate for the coating deposition. Prior to the spraying process, the substrate was blasted with silicon carbide grits in order to increase the adhesion strength of the coating to the substrate.

B. Plasma Spray Coating

P550 Metallization Atmospheric plasma spraying system was used to deposit the TiO₂ coating. N₂ carrier gas flow rate was 4 l/min. Powder feed rate was set for 8 g/min, with Argon being used as the primary plasma gas. Arc current used for plasma was 400 A. Four sets of spray parameters as indicated in Table 1 were employed to provide different spray coatings.

¹M. Bozorgtabar is with the Majlesi Branch, Islamic Azad University, Isfahan, Iran (phone: 98(3355452290-4; fax:98(311)6638984; e-mail:mbozorgtabar@iaumajlesi.ac.ir).

²M. Rahimipour is with the Materials & Energy Research Center, P.O. Box 14155-4777, Tehran, Iran (e-mail:m-rahimi@merc.ac.ir)

³M. Salehi is with Isfahan University of Technology, Isfahan 84154, Iran (e-mail:salehi@hotmail.co.uk)

⁴M. Jafarpour is with the Mobarakeh Steel Company, P.O. Box 84815-161, Isfahan, Iran.

TABLE I
PLASMA SPRAY CONDITIONS

Samples	Ar flow rate (l/min)	stand-off distance (mm)
A1	28.5	50
A2	36	50
A3	28.5	80
A4	36	80

C. Characterization

The morphology of powders and the microstructure of surface and cross section of coatings were examined using a S360 Cambridge scanning electron microscope (SEM). The diffused reflection absorption spectra (DRS) were performed on a Shimadzu UV-3100PC scanning spectrophotometer equipped with a diffuse reflectance accessory. The absorption intensity was calculated from the Kubelka–Munk equation as:

$$f(R) = (1-R)^2 / 2R \quad (1)$$

Where $f(R)$ is Kubelka – Munk value and R is diffuse reflection of the coating. The $f(R)$ is proportional to the absorption coefficient.

Fourier transform infrared spectra (FT-IR) were recorded with a Fourier transform infrared spectrometer (BRUKER, VECTOR 33). Samples (softly scraped-off from the substrate) were gently ground and diluted in nonabsorbent KBr matrices (2% by weight). All DRIFT spectra are shown in transition units and obtained under atmospheric conditions.

III. RESULTS AND DISCUSSION

A. Coatings morphology

Figures 1 and 2 present the SEM of the plasma-sprayed coatings, which shows the typical surface and cross section microstructures of coatings. The micrographs show that the coatings are not very dense; i.e. they contain many holes. It also can be seen that there are two kinds of structures in the coating; one is the continuous molten phase, and the other is the loose microstructure which has resulted from the existence of the non-molten or semi-molten starting powders in the spraying process. It is noted that in the coating with the higher fuel value more melted microstructure and porosity can be detected.

During the plasma spraying, the working fluid (plasma flame) has a high enthalpy density, which is controlled by the arc current conditions [22]. The higher current offers a higher enthalpy density, which influences the different melting phenomena of the starting powders. The TiO₂ powders melted more fully with the increasing fuel flow rate. The partly- and un-melted particles that exist is a phenomenon which will be of benefit to increase the specific surface, and thus improve the photo-catalytic activity of the sprayed coatings [23]. Coatings with many holes and cracks also have an important beneficial influence on the photo-catalytic activity.

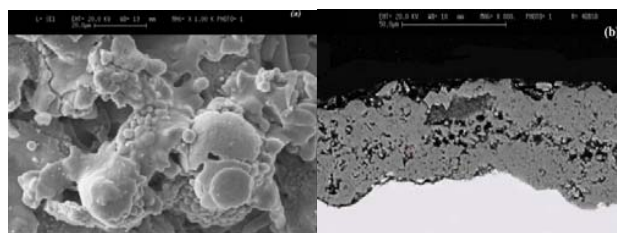


Fig.1 (a) SEM surface topography and (b)SEM cross section micrograph of TiO₂ plasma sprayed coating with 28.5 l/min Argon flow rate and 80 mm stand-off distance (A3)

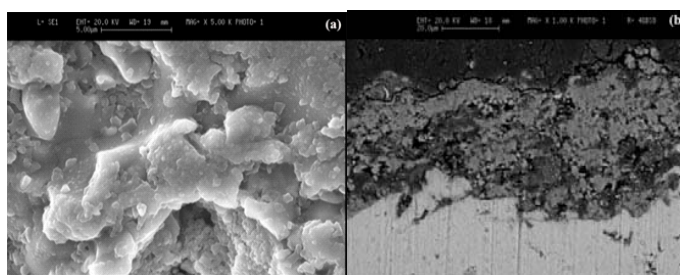


Fig. 2 (a) SEM surface topography and (b)SEM cross section micrograph of TiO₂ plasma sprayed coating with 36 L/min Argon flow rate and 80 mm stand-off distance (A4)

B. Energy absorbance of feedstock powders and sprayed coatings

The diffuse reflectance of sprayed coatings was investigated using the Shimadzu UV-3100PC scanning spectrophotometer. Generally, the photo-catalytic activity increases with the increasing of light absorptive capacity. The Kubelka–Munk values (calculated by Kubelka-Munk function $f(R)$) of sprayed coatings fall into the wavelength range of 340 to 400 nm according to Fig.3, which means that sprayed coatings have a lower photo-absorptive ability in the visible spectral range. Kubelka–Munk values of the A3 coating with higher anatase content in the experimental light wavelength of 360 nm are higher than the A1, A4 and A2 coatings which, means that more UV irradiation energy can be utilized. It can be seen clearly that light absorption at the wavelength from 400 nm to 800 nm is closely for the four types of coatings, but increasing largely in the shorter wavelengths, especially from 380 nm to 410 nm, which is near to TiO₂ band-gap edge wavelengths. In general, the onset of band-gap absorption of anatase TiO₂ is estimated 387 nm, which corresponds to 3.2 eV; the onset of band-gap absorption of rutile TiO₂ is 417 nm, which corresponds to 3.0 eV [24]. The feedstock powder used here contains 75% anatase and 25% rutile, and the onset of its band gap absorption is estimated 405-410 nm, which corresponding to ca. 3.08 eV. In the range of wavelength lower than 380 nm, UV light can be absorbed effectively by TiO₂. The absorption ledge of coating with higher rutile ratio content has red shift to larger wavelength and coatings with lower rutile content had blue shift.

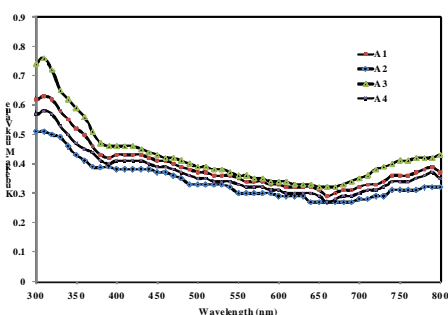


Fig.3. Photo-absorption of TiO₂ plasma sprayed coatings at different process parameters as indicated in Table I

C. Results of FT-IR

The FT-IR spectra in Fig. 4 for the obtained samples show that the surface-adsorbed water and hydroxyl groups exist, as shown by the appearance of broad peaks at 3400 and 1638 (1/cm). It is evident that the plasma spray has reduced the adsorption of the surface hydroxyl groups. The intensity of these peaks decreased in the A2 and A4 samples more than in the A1 and A3 samples, indicating the diminishing effect of the surface hydroxyl groups. This decrease is probably due to the smaller surface site of the larger crystalline size. The broad peak in the range of 400–1000 (1/cm) can be attributed to the anatase phase [25, 26].

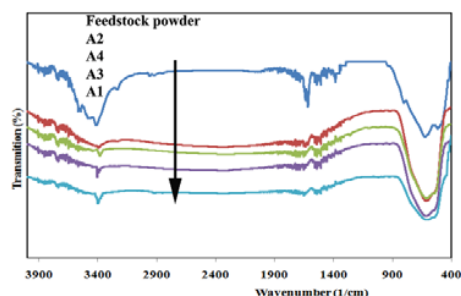


Fig.4 FT-IR spectra of feedstock powder and TiO₂ plasma sprayed coatings at different process parameters as indicated in Table I

IV. CONCLUSION

P25/20 TiO₂ nano-powder was atmospheric plasma sprayed on to stainless steel substrates under various spray. The effects of spraying conditions on microstructure, crystal structure, photo-adsorption energy and surface feature of prepared coatings were investigated. The results are summarized as follows:

- (1) When plasma spraying was carried out under the conditions of higher heat with higher Argon flow rate, the phase transformation of anatase to rutile increased and so the anatase content in coating decreased, respectively.
- (2) The fraction of melted TiO₂ particles in microstructure was higher with increasing Argon flow rate.
- (3) The surface characteristics of sprayed coatings showed that they have an anatase phase with a lower surface water-absorbed and hydroxyl group than feedstock powder and that

their surface water-absorbed and hydroxyl group vary according to the various spray conditions.

- (5) Visible light adsorption of all coatings was low according to their Kubalko-Munk values.

REFERENCES

- [1] M. Pourmand, N. Taghavinia, Materials Chemistry and Physics 107, 449- 455 (2008).
- [2] A. Orendorz, A. Brodyanski, J. Lo'sch, L.H. Bai , Z.H. Chen , Y.K. Le , C. Ziegler, H.Gnaser, Surface Science 601, 4390-4394 (2007).
- [3] Y. CUI, H. DU , L. WEN, J. Mater. Sci. Technol. 24, 5 (2008).
- [4] F. Sayilkan , M. Asiltu'rk, P. Tatar , N. Kiraz, S. S. Sener , E. Arpac., H. Sayilkan, Materials Research Bulletin 43, 127-134 (2008).
- [5] H. Shon, S. Phuntsho, Y. Okour, D.L. Cho, K. S. Kim, H.J. Li, S. Na, J. B. Kim, J.H. Kim, J. Korean Ind. Eng. Chem. 19, 1-16 (2008).
- [6] S.C. Lee, C.W.Lee, S. C. Lee, J.S. Lee, Materials Letters 62, 564-566 (2008).
- [7] N. Wetchakun, S. Phanichphant, Current Applied Physics 8, 343-346 (2008)
- [8] H. Jensen, K. D. Joensen, J.E. Jrgensen, J. S. Pedersen and E. G. Sgaard, Journal of Nanoparticle Research 6, 519-526 (2004).
- [9] J.M. Peralta-Hern', J. Manr'iquez, Y. Meas-Vong, F. J. Rodr'iguez, T. W. Chapman, M. Maldonado, L. A. God'inez, Journal of Hazardous Materials 147, 588-593 (2007).
- [10] P. Supphasirongjaroen, P. Praserttham, J. Panpranot, D. N. Ranong, O. Mekasuwandumrong, Chemical Engineering Journal 138, 622-627 (2008) .
- [11] D. Li, H. Haneda, S. Hishita, N. Ohashi, Res. Chem. Interme. 31, 331-341 (2005).
- [12] S.N. Hosseini, S.M. Borghei, M. Vossoughi, N. Taghavinia, Applied Catalysis B: Environmental 74, 53-62 (2007).
- [13] L. Ko'ro'si, A. Oszko, G. Galba'cs, A. Richardt, V. Zo'llmer, I. De'ka'ny, Applied Catalysis B: Environmental 77, 175-183 (2007).
- [14] G.J. Yang, C. J. Li, Y. Y. Wang, C. X. Li, Materials Letters 62, 1670-1672 (2008) .
- [15] G. Bolelli, V. Cannillo, L. Lusvardi, F. P. Mantini, E. Gualtieri, C. Menozzi, Materials Letters 62, 1557-1560 (2008).
- [16] Z. Yi, C. Guofeng, W. Ma, W. Wei, Progress in Organic Coatings 61, 321-325 (2008).
- [17] Q. Yu, C. Zhou, X. Wang, Journal of Molecular Catalysis A: Chemical 283, 23-28 (2008).
- [18] S. O. Chwa, D. Klein, F. L. Toma, G. Bertrand, H. Liao, C. Coddet, A. Ohmori, Surface & Coatings Technology 194, 215- 224 (2005).
- [19] T. Kanazawa, A. Ohmori, Surface & Coatings Technology 197, 45- 50 (2005).
- [20] F. L. Toma, G. Bertrand, S. O. Chwa, D. Klein, H. Liao, C. Meunier, C. Coddet, Materials Science and Engineering A 417, 56-62 (2006).
- [21] F. Ye, A. Ohmori, Surface and Coatings Technology 160, 62-67 (2002).
- [22] M. Gaona, R.S. Lima, B.R. Marple, journal of materials processing technology 198, 426-435 (2008) .
- [23] Y. Zhai, Y. Gao, F. Liu, Q. Zhang, G. Gao, Materials Letters 61, 5056-5058 (2007).
- [24] M. S. Wong, S. W. Hsu, K. K. Rao, C. P. Kumar, Journal of Molecular Catalysis A: Chemical 279, 20-26, 2008.
- [25] D. Zhao, T. Peng, M. Liu, L. Lu, P. Cai, Microporous and Mesoporous Materials 114, 166-174 (2008).
- [26] S. Liu, X. Chen, Journal of Hazardous Materials 152, 48-55 (2008).